Oblique triangular antiferromagnetic phase in $CsCu_{1-x}Co_xCl_3$

T. Ono,* T. Kato,† and H. Tanaka
Department of Physics, Tokyo Institute of Technology, Tokyo 152-8551, Japan

A. Hoser, N. Stüßer, and U. Schotte
Hahn-Meitner-Institut, Glienicker Straße 100, D-14109 Berlin, Germany

(Received 12 July 2000; published 24 May 2001)

The spin-$\frac{1}{2}$ stacked triangular antiferromagnet $CsCu_{1-x}Co_xCl_3$ with $0.015<x<0.032$ undergoes two phase transitions at zero field. The low-temperature phase is produced by doping a small amount of Co^{2+}. In order to investigate the magnetic structures of the two ordered phases, the neutron elastic scattering experiments have been carried out for the sample with $x\approx0.03$. It is found that the intermediate phase is identical to the ordered phase of $CsCuCl_3$, and that the low-temperature phase is an oblique triangular antiferromagnetic phase in which the spins form a triangular structure in a plane tilted from the basal plane. The tilting angle, which is 42° at $T=1.6$ K decreases with increasing temperature, and becomes zero at the lower transition temperature $T_{N2}=7.2$ K. An off-diagonal exchange term is proposed as the origin of the oblique phase.

DOI: 10.1103/PhysRevB.63.224425 PACS number(s): 75.25.+z, 75.30.Kz

I. INTRODUCTION

Among the group of antiferromagnets which have a hexagonal ABX_3 triangular structure, many experimental and theoretical investigations of $CsCuCl_3$ have been performed by several authors,[1–4] due to the remarkable features of this compound. Since the Cu^{2+} ion is Jahn-Teller active, $CsCuCl_3$ undergoes a structural phase transition at $T_t=423$ K, where Jahn-Teller-distorted octahedral $CuCl_6$ become ordered such that their longest axes form a helix along the c axis with a repeat length of six.[5–7] The low-symmetry crystal structure produces the antisymmetric interaction of the Dzyaloshinsky-Moriya (DM) type between the adjacent spins in the chain with the D vector parallel to the c direction. The exchange interactions along and between the chains are ferromagnetic and antiferromagnetic, respectively, and their values have been evaluated as $J_0/k_B=28$ K and $J_1/k_B=-4.9$ K,[8,9] in the definition of $\mathcal{H}=-\Sigma_{\langle i,j\rangle}2J_{ij}S_i\cdot S_j$. The magnetic phase transition occurs at $T_N=10.5$ K.[10,11] In the ordered state, spins lie in the basal plane and form the 120° structure, while along the c direction, a long-period (about 71 triangular layers) helical incommensurate arrangement is realized due to the competition between the ferromagnetic interaction and the DM interaction along the chain.

Since the magnitude of spin on Cu^{2+} is $S=\frac{1}{2}$, quantum fluctuations are important when one describes the magnetic behavior in the magnetic field.[12] In particular, the magnetization process with a strong field often reveals quantum effects in the form of macroscopic phenomena. Using quantum Monte Carlo calculations or the spin wave theory, for the 2D triangular antiferromagnet (TAF) in the isotropic limit, it is predicted that the magnetization plateau appears at around one-third of the saturation value M_s.[13,14] According to these predictions, when the external field H is applied parallel to the c axis, 2D TAF undergoes a successive phase transition, as shown in Fig. 1, from the (b) low-field coplanar, to the (c) collinear to the (d) high-field coplanar structure, in that order. In the field region where the magnetization plateau appears, the spin structure corresponds to structure (c). For $CsCuCl_3$, instead of a plateau, there is a small magnetization jump around $M_s/3$ when the field is applied parallel to the c axis. This is understood to result from the competition between weak planar anisotropy and quantum fluctuation, i.e., the structure in Fig. 1(a) is stabilized by the planar anisotropy up to $H_c=12.5$ T$>H_s/3$ and the structure in Fig. 1(d) is stabilized by quantum fluctuation above $H>H_c$, skipping structures (b) and (c). The existence of the plateau at $M=M_s/3$ is strongly dependent on the magnetic anisotropy. Recently, Honecker *et al.*[15] argued that the proper combination of the interchain interaction $|J_1|/J_0$ and XXZ anisotropy $\Delta=J^z/J^{xy}$ allows the existence of the plateau at $M=M_s/3$, even in the region of $\Delta<1$ (small planar anisotropy). Here, $J^\alpha(\alpha=z$ and $xy)$ are anisotropic exchange constants defined by $\mathcal{H}=-2\Sigma_i[J^{zz}_{i\,i+1}S^z_iS^z_{i+1}+\frac{1}{2}J^{xy}_{i\,i+1}(S^+_iS^-_{i+1}+S^-_iS^+_{i+1})]$. Therefore, it is very interesting to study how the phase transition changes when the macroscopic anisotropy of $CsCuCl_3$ is controlled. Because of this motivation, we have synthesized the mixed system $CsCu_{1-x}Co_xCl_3$ with 1.5–3.2% of Co^{2+} ions in the concentration x, since $CsCoCl_3$ is known to be a pseudospin-$\frac{1}{2}$ TAF with easy-axis anisotropy.[16,17]

In our previous paper,[18] we reported the results of the magnetic measurements for $CsCu_{1-x}Co_xCl_3$ with $x<0.032$ and the magnetic phase diagram for temperature versus magnetic field up to 7 T. Figure 2 shows the magnetic phase diagram for the external field versus temperature for the

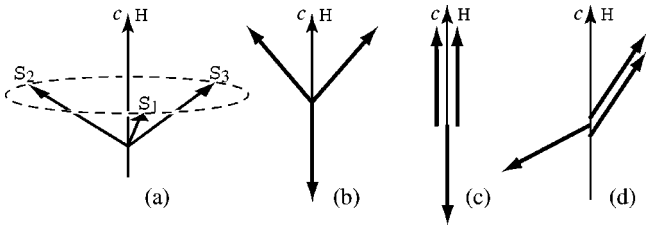

FIG. 1. Spin structures of 2D TAF in the magnetic field. (a) Umbrella-type structure, (b) low-field coplanar structure, (c) collinear structure, and (d) high-field coplanar structure.

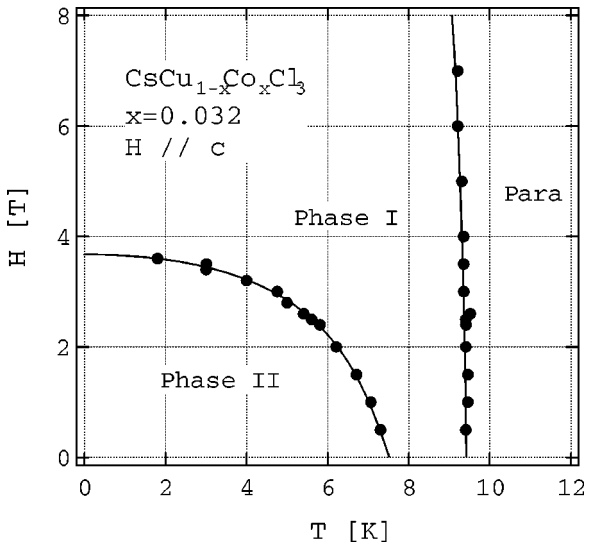

FIG. 2. The magnetic phase diagram of $CsCu_{1-x}Co_xCl_3$ with $x=0.32$ for the magnetic field parallel to the c axis.

sample with $x=0.032$ in a field parallel to the c axis.

Before the magnetization measurements, our first speculation was that when Co^{2+} ions are doped to reduce the planar anisotropy, structure (a) is realized in the ground state at zero field, and strucutre (b), which benefits quantum fluctuation, might appear in the field region of $H \leqslant H_s/3$.

On the other hand, the experimental results of the magnetization measurements indicate that the spin structure of phase II is stabilized with the help of the axial anisotropy. With decreasing Co^{2+} concentration x, the area of phase II is reduced and then disappears when $x \leqslant 0.005$. Thus it is reasonable to infer that the spin structure in the intermediate phase I is identical to that of $CsCuCl_3$. However, within the magnetic measurements the spin structures of the intermediate phase and low-temperature phase cannot be determined. Therefore, in order to determine the spin structures of these two phases, we have performed neutron scattering experiments for the sample with $x \approx 0.03$.

II. EQUIPMENT

Single crystals of $CsCu_{1-x}Co_xCl_3$ were prepared by the Bridgman method from the melt of single crystals of $CsCuCl_3$ and $CsCoCl_3$. The details of the sample preparation have been described in the previous paper.[18]

Neutron scattering experiments were performed at the BER II Research Reactor of the Hahn-Meitner-Institute using the triple axis spectrometer $E1$ operated in the double-axis mode. The incident neutron energy was fixed at $E_i = 13.9$ meV by Bragg reflection at the pyrolytic graphite monochromator, and the horizontal collimations are chosen to be 40′-40′-40′-open. A single crystal of $CsCu_{1-x}Co_xCl_3$ with $x \approx 0.03$ was used. We label this sample $CsCu_{0.97}Co_{0.03}Cl_3$. The sample is in the shape of a triangular prism 5 mm in width and 15 mm in length. The sample was mounted in the cryostat with its [1, 1, 0] and [0, 0, 1] axes in the scattering plane.

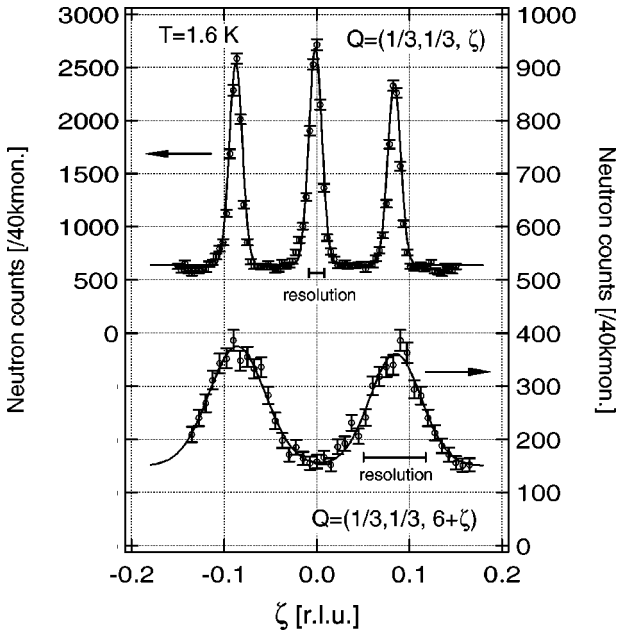

FIG. 3. Scans along $Q=(1/3,1/3,\zeta)$ with (a) $\zeta=0$ and (b) $\zeta=6$. Solid lines represent the results of Gaussian fitting. Horizontal bars denote the instrumental resolution.

III. RESULTS

From the previous magnetic measurements, the sample with $CsCu_{0.97}Co_{0.03}Cl_3$ is known to undergo phase transitions at $T_{N1} \simeq 9.5$ K and $T_{N2} \simeq 7.2$ K. First, we confirmed that the crystal structure of the present system is identical to that of pure $CsCuCl_3$, i.e., that there are nuclear Bragg peaks at $(00l)$ with $l=0 \sim 6$, which is indicative of the sixfold helix. From the nuclear Bragg peaks at (1, 1, 0) and (0, 0, 6), the lattice constants at helium temperature were determined to be $a=7.137$ Å and $c=18.036$ Å.

Figure 3 shows the scans along $Q=(1/3,1/3,\zeta)$ and $(1/3,1/3,6+\zeta)$ at $T=1.6$ K for phase II. The magnetic Bragg scattering consists of one central peak at $\zeta=0$ and two side peaks at $\zeta=\pm\delta$ with $\delta=0.084$. The temperature dependence of the scan profile (see Fig. 4) shows that possible changes of δ are negligible, similar to pure $CsCuCl_3$. The possibility that the central peak and the side peaks are due to different magnetic domains is excluded, because the temperature variations of their intensities are strongly correlated, as shown in Fig. 5. We see that the magnetic unit cell is enlarged by $\sqrt{3}\times\sqrt{3}$ in the basal plane, which is characteristic of the triangular spin arrangement. The side peaks indicate that the helical spin structure is realized along the c axis. The value of δ corresponds to the period of the helix. The period is evaluated as $6/\delta=71.4$ Cu sites, which is almost the same value as that in $CsCuCl_3$, i.e., 70.6 Cu sites.[10]

It is noteworthy that in the present system, the magnetic Bragg peak is observed at $Q=(1/3,1/3,0)$, which is absent in $CsCuCl_3$. On the other hand, around (1/3, 1/3, 6), the central peak is very weak as compared with the side peaks (see Fig. 3). The difference in Bragg width for each scattering profile is only due to the instrumental resolution. Since the angle between the scattering vector and the c^*-axis is 90° for Q

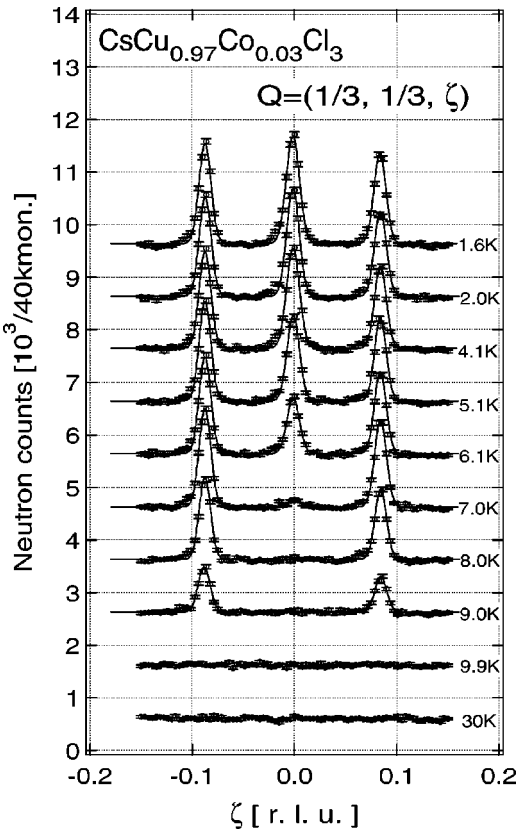

FIG. 4. Scans along the c^* axis around $Q=(1/3,1/3,0)$ at various temperatures.

$=(1/3,1/3,0)$ and 15.7° for $Q=(1/3,1/3,6)$, the c-axis component of spins is much less visible around the (1/3, 1/3, 6) reflection than around the (1/3, 1/3, 0) reflection. On the other hand, the basal plane component of spins make a larger

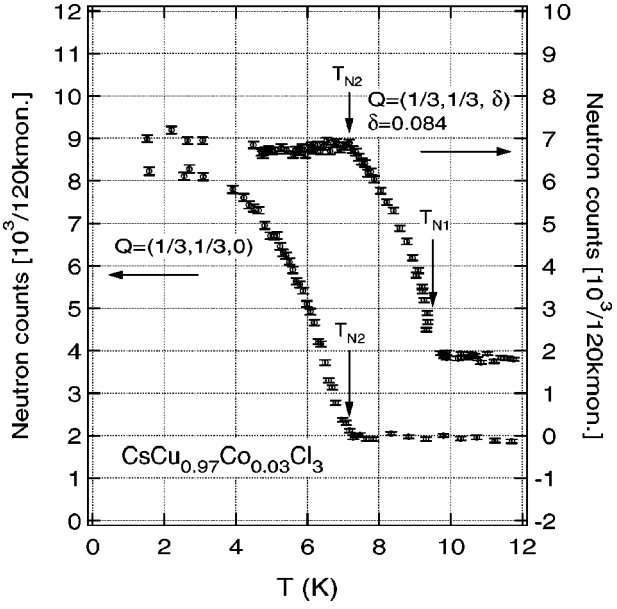

FIG. 5. Magnetic Bragg intensities at $Q=(1/3,1/3,0)$ and (1/3,1/3,0.084) as a function of temperature. Néel temperatures are indicated by arrows.

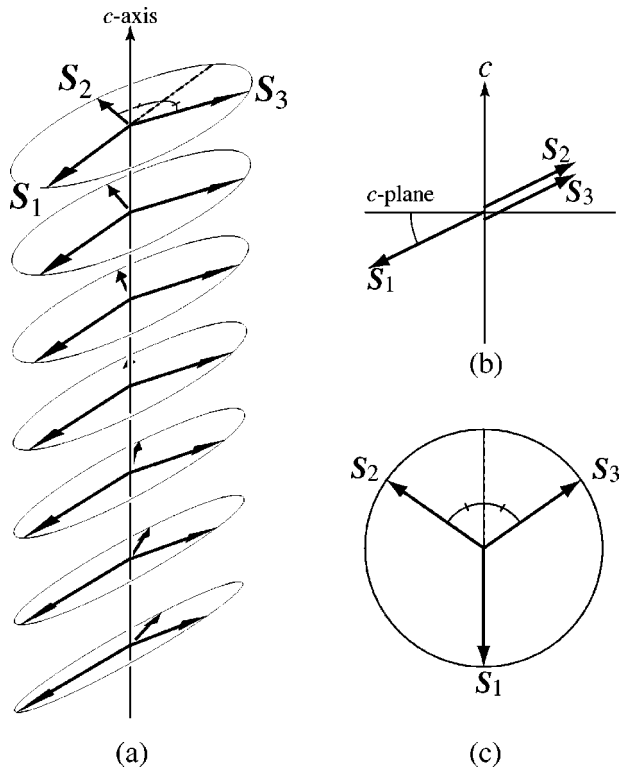

FIG. 6. (a) Oblique triangular antiferromagnetic structure in the low-temperature phase. Tilted spin planes represented by circles are stacked along the c axis, forming a helix with a pitch of 5°. (b) The angle ϕ indicates the tilt of the spin plane from the c plane. (c) The angle γ is half the angle between S_2 and S_3.

contribution to the magnetic reflections around (1/3, 1/3, 6). Thus, it is deduced that the central peaks originate from the c-axis component of spins, while the basal plane component gives rise to the side peaks, as in $CsCuCl_3$. We refer to a plane spanned by the spins on a triangular lattice as the *spin-plane* in this paper. The present result leads us to conclude that phase II is an oblique triangular phase in which the spin plane is tilted at angle ϕ from the basal plane [see Fig. 6(a) and 6(b)]. The spin planes are stacked along the c-axis, forming a helix with a pitch of $360\times\delta/6-5°$. (It should be noted that this model of spin structure which we present here is the average structure in the macroscopic view. The local spin structure may reflect the inhomogeneity of the crystal.)

It is natural to consider that the spin structure in each spin plane is close to the 120° structure, because there is no anisotropy which is strong enough to significantly deform the 120° structure or lift the moments from the spin plane. In order to take account of a slight deformation from the 120° structure, the angle 2γ between the spins $\boldsymbol{S}_2$ and $\boldsymbol{S}_3$ is adopted as a variable parameter, as illustrated in Fig. 6(c). Under the assumption that the thermal averages of spins on all sublattices are the same, the integrated intensity of the magnetic Bragg peaks for $Q=(h,h,\zeta)$ with $h=n/3$ is given by

$$I\propto|f(Q)|^2L(\theta)|F(h,h,\zeta)|^2,$$

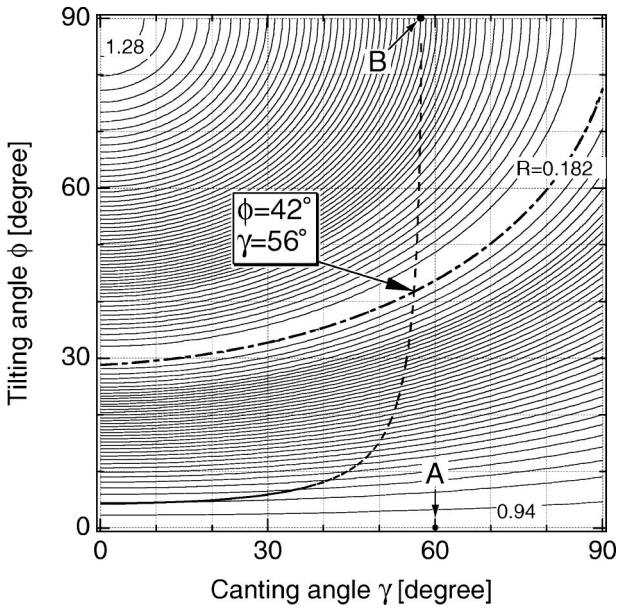

FIG. 7. Contour plot of the reliability factor R as a function of angles γ and ϕ. Dot-dashed line indicates the minimized R factor $R=0.182$. Dashed line indicates the line which satisfies Eq. (5).

$$L(\theta)=\cos\left(\frac{\pi}{2}-\theta-\arccos\sqrt{\frac{a^2\zeta^2}{4c^2h^2+a^2\zeta^2}}\right) \tag{1}$$

and $I=0$ for integer h, where θ is half the scattering angle, $L(\theta)$ is the Lorentz factor for the parallel scans, $f(Q)$ is the magnetic form factor and a and c are lattice constants. The values of $f(Q)$ were taken from Ref. 19. $F(h,h,\zeta)$ is the magnetic structure factor. Due to the long-period helical spin structure along the c-axis, the component in the a-b plane and the c-axis component of the spins give Bragg peaks at $\zeta=\pm\delta$ and $\zeta=0$, respectively. The structure factors for the planar component F_{ab} and the axial component F_c are described as

$$|F_{ab}(hh\zeta)|^2=d^2_{(hh\zeta)}\left\{2\left(\frac{h}{a}\right)^2+\left(\frac{\zeta}{c}\right)^2\right\}\times\{(1+\cos\gamma)^2\cos^2\phi+3\sin^2\gamma\}, \tag{2}$$

$$|F_c(hh\zeta)|^2=d^2_{(hh\zeta)}\left(\frac{2h}{a}\right)^2(1+\cos^2\gamma)\sin^2\phi, \tag{3}$$

where $d_{(hh\zeta)}$ is the spacing of the (h,h,ζ) lattice plane. Integrated Bragg intensities are calculated for various angles of ϕ and γ. In Fig. 7 the variation of the reliability factor R given by

$$R=\sum_{h,h,\zeta}|I_{\rm calc}(h,h,\zeta)-I_{\rm obs}(h,h,\zeta)|\Big/\sum_{h,h,\zeta}I_{\rm obs}(h,h,\zeta)$$

is represented as a contour map. We see that the R-factor has the same minimum value along the dot-dashed line in Fig. 7. With decreasing tilting angle ϕ, the canting angle γ which gives the minimum R-factor rapidly decreases and becomes zero when $\phi=29.2°$. Since the magnetic structure could not be determined uniquely from only the magnetic Bragg intensities, the value of the spontaneous magnetization along the c-axis determined from magnetization measurements (see Fig. 2 in Ref. 18) is necessary to give a conclusive answer. For the oblique triangular structure, each sublattice spin is described as

$$S_1=S(\cos\phi,0,-\sin\phi),$$

$$S_2=S(-\cos\gamma\cos\phi,-\sin\gamma,\cos\gamma\sin\phi),$$

$$S_3=S(-\cos\gamma\cos\phi,\sin\gamma,\cos\gamma\sin\phi). \tag{4}$$

Hence, the spontaneous magnetization $M_{\rm sp}$ per site is given by

$$M_{\rm sp}=\frac{2\cos\gamma-1}{3}\sin\phi[\mu_{\rm B}/\text{magnetic ion}]. \tag{5}$$

In Fig. 7, the dashed line corresponds to $M_{\rm sp}=0.025\ \mu_{\rm B}$ which was obtained through the previous magnetization measurements.[18] From the values at the intersection of dashed and dot-dashed lines, the angles ϕ and γ are obtained as $(\phi,\gamma)=(42°,56°)$.

In Table I, we show the experimental and calculated intensities of the Bragg peaks around $Q=(1/3,1/3,0)$, (1/3, 1/3, 6) and (2/3, 2/3, 0), together with the calculated intensities which correspond to the A and B points in Fig. 7. Experimental and calculated intensities are normalized for the total intensities of central and side peaks around (1/3, 1/3, 0). The spin structure of $CsCuCl_3$ corresponds to the case of $\phi=0°$ and $\gamma=60°$ which is indicated by A in Fig. 7. We see from Table I that the spins form the triangular structure neither in the c-plane, nor in the plane including the c axis, but in a plane tilted from the c-plane by angle $\phi=42°$ and that the triangular spin structure ($\gamma=56°$) is close to the 120° spin structure. The difference between the observed and calculated values of the scattering intensities arise from the fact that we did not taking into account the variation of the magnitude of S for each sublattice.

As shown in Fig. 5, with increasing temperature, the intensity of the central peak decreases and disappears at $T_{\rm N2}=7.2$ K. On the other hand, the intensity of the side peak is almost constant up to $T_{\rm N2}$, and decreases rapidly, and becomes zero at $T_{\rm N1}=9.5$ K. Both phase transitions are sharp, which indicates good homogeneity of the sample. From the present result, we see that the tilt angle ϕ decreases with increasing temperature, and becomes zero at $T_{\rm N2}$. Thus, we can deduce that phase I between $T_{\rm N2}$ and $T_{\rm N1}$ is identical to the ordered phase of $CsCuCl_3$, which is consistent with the fact that Co^{2+} doping produces phase II in the low-temperature, low-field region in the ordered state of $CsCuCl_3$, and that its area increases with increasing Co^{2+} concentration x.

$CsCuCl_3$ has that a weak planar anisotropy, while $CsCoCl_3$ is an Ising spin system.[16] Phase transitions in the random spin systems with competing anisotropies have been investigated in $Fe_{1-x}Co_xCl_2$[20] and $Fe_{1-x}Co_xCl_2\cdot 2H_2O$[21] by means of neutron scattering. Both systems undergo two phase transitions, which are characterized by the orderings of

TABLE I. Experimental and calculated intensities of several magnetic Bragg reflections in $CsCu_{1-x}Co_xCl_3$ with $x=0.03$ at $T=1.6$ K. They are normalized to the total peak intensities around the $Q=(1/3,1/3,0)$ reflection. The calculated intensities at A and B points in Fig. 7 are also shown for comparison.

(h,h,ζ)	I_{obs}	$I_{calc}\begin{pmatrix}\phi=42°\\ \gamma=57°\end{pmatrix}$	$I_{calc}(A)\begin{pmatrix}\phi=0°\\ \gamma=60°\end{pmatrix}$	$I_{calc}(B)\begin{pmatrix}\phi=90°\\ \gamma=57.49°\end{pmatrix}$
$(\frac{1}{3},\frac{1}{3},-\delta)$	0.324	0.306	0.497	0.155
$(\frac{1}{3},\frac{1}{3},0)$	0.384	0.384	0	0.689
$(\frac{1}{3},\frac{1}{3},\delta)$	0.292	0.310	0.503	0.156
$(\frac{1}{3},\frac{1}{3},6-\delta)$	0.210	0.230	0.373	0.116
$(\frac{1}{3},\frac{1}{3},6)$	0.012	0.011	0	0.019
$(\frac{1}{3},\frac{1}{3},6+\delta)$	0.186	0.226	0.366	0.114
$(\frac{2}{3},\frac{2}{3},-\delta)$	0.171	0.266	0.432	0.135
$(\frac{2}{3},\frac{2}{3},0)$	0.252	0.330	0	0.573
$(\frac{2}{3},\frac{2}{3},+\delta)$	0.172	0.266	0.432	0.134
		$R=0.182$	$R=0.947$	$R=0.598$
$M_{sp}[\mu_B/\text{ion}]$	0.025	0.025	0	0.025

two spin components. In $Fe_{1-x}Co_xCl_2$, the ordering of one spin component is drastically altered by the ordering of the other component, so that the lower-temperature transition is rather smeared. On the other hand, in $Fe_{1-x}Co_xCl_2\cdot 2H_2O$, two phase transitions are sharp, and two order parameters are decoupled. $CsCu_{0.97}Co_{0.03}Cl_3$ differs from the above two in the nature of the ordering. In the present system, the basal plane component of spins orders first at T_{N1} and then the *c*-axis component orders at T_{N2}, so that the oblique triangular spin structure is realized. Both phase transitions are fairly sharp, and neither components is decoupled, i.e., the growth of the basal plane component of spins below T_{N2} is suppressed due to the growth of the *c*-axis component which is equivalent to the increase of tilting angle ϕ. The present system is the first example of a system that undergoes a definite phase transition to the oblique spin phase. The mechanism seems not to be explained by only competing anisotropies, because mixed triangular antiferromagnetic systems with axial and planar anisotropies, such as $Rb_{1-x}K_xNiCl_3$[22] and $CsMn(Br_xI_{1-x})_3$,[23,24] exhibit neither the mixed ordered phase nor the oblique phase.

In $CsCuCl_3$, the off-diagonal exchange term of the form

$$\mathcal{H}_{od}=J_{ij}^{zx}(S_i^zS_j^x+S_i^xS_j^z)+J_{ij}^{zy}(S_i^zS_j^y+S_i^yS_j^z) \qquad (6)$$

is allowed, because the elongated axes of $CuCl_6$ octahedra are canted from the *c* axis, so that the local symmetry is lower than the trigonal one. Here we take the *z* axis parallel to the *c* axis and the *x* and *y* axes in the basal plane. The off-diagonal exchange term has been proposed in order to interpret the nature of the mixed ordered state in $Fe_{1-x}Co_xCl_2$.[20,25] Recently, Pleimling[26] discussed the ordering of the perpendicular spin component in the Ising-like system $FeBr_2$ on the basis of the off-diagonal exchange term. Due to the off-diagonal term, the ordering of the basal plane component of spins can induce the ordering of the *c*-axis component. We suggest that the doping of small amounts of Co^{2+} ions suppresses the planar anisotropy on average, so that the effect of the off-diagonal term is enhanced. However, whether the orderings of both components occur simultaneously or separately, as observed in the present system, is unclear.

Currently, a theoretical attempt to clarify the sign and magnitude of the exchange interaction between Cu^{2+} and Co^{2+} ions and the microscopic spin structure in the oblique phase is being made by another group.[27]

IV. CONCLUSIONS

We have performed elastic neutron scattering experiments on the triangular antiferromagnetic system $CsCu_{0.97}Co_{0.03}Cl_3$ which undergoes two phase transitions at $T_{N1}=9.5$ K and $T_{N2}=7.2$ K. It was found that the low-temperature phase is an oblique triangular antiferromagnetic phase with the spin-plane tilted from the basal plane, and that the intermediate phase is identical to the ordered phase of $CsCuCl_3$. We suggest that the off-diagonal exchange interaction gives rise to the oblique phase in the present system.

ACKNOWLEDGMENTS

The authors wish to thank K. D. Schotte and H. Shiba for useful dicussions.

*Email address: o-toshio@lee.phys.titech.ac.jp
†Present address: Faculty of Education, Chiba University, 263-8522 Chiba, Japan

[1] H. Nojiri, K. Takahashi, T. Fukuda, M. Fujita, M. Arai, and M. Motokawa, Physica B **241-243**, 210 (1998).
[2] T. Werner, H.B. Weber, J. Wosnitza, A. Kelnberger, M. Meschke, U. Schotte, N. Stüßer, Y. Ding, and M. Winkelmann, Solid State Commun. **102**, 609 (1997).
[3] U. Schotte, A. Kelnberger, and N. Stüßer, J. Phys.: Condens. Matter **10**, 6391 (1998).
[4] A.E. Jacobs and T. Nikuni, J. Phys.: Condens. Matter **10**, 6405 (1998).
[5] A.W. Schlueter, R.A. Jacobson, and R.E. Rundle, Inorg. Chem. **5**, 277 (1966).
[6] C.J. Kroese, W.J.A. Maaskant, and G.D. Verschoor, Acta Crystallogr., Sect. B: Struct. Crystallogr. Cryst. Chem. **30**, 1053 (1974).
[7] S. Hirotsu, J. Phys. C **10**, 967 (1977).
[8] Y. Tazuke, H. Tanaka, K. Iio, and K. Nagata, J. Phys. Soc. Jpn. **50**, 3919 (1981).
[9] H. Tanaka, U. Schotte, and K.D. Schotte, J. Phys. Soc. Jpn. **61**, 1344 (1992).
[10] K. Adachi, N. Achiwa, and M. Mekata, J. Phys. Soc. Jpn. **49**, 545 (1980).
[11] H.B. Weber, T. Werner, J. Wosnitza, H. von Löhneysen, and U. Schotte, Phys. Rev. B **54**, 15 924 (1996).
[12] T. Nikuni and H. Shiba, J. Phys. Soc. Jpn. **62**, 3268 (1993).
[13] H. Nishimori and S. Miyashita, J. Phys. Soc. Jpn. **64**, 4448 (1986).
[14] A.V. Chubukov and D.I. Golosov, J. Phys.: Condens. Matter **3**, 69 (1991).
[15] A. Honecker, M. Kaulke, and K.D. Schotte, Eur. Phys. J. B **15**, 423 (1999).
[16] M.F. Collins and O.A. Petrenko, Can. J. Phys. **75**, 605 (1997) and references therein.
[17] M. Mekata and K. Adachi, J. Phys. Soc. Jpn. **44**, 806 (1978).
[18] T. Ono, H. Horai, and H. Tanaka, J. Phys.: Condens. Matter **12**, 975 (2000).
[19] R.E. Watson and A.J. Freeman, Acta Crystallogr. **14**, 27 (1961).
[20] P. Wong, P.M. Horn, R.J. Birgeneau, and G. Shirane, Phys. Rev. B **27**, 428 (1983).
[21] K. Katsumata, H. Yoshizawa, G. Shirane, and R.J. Birgeneau, Phys. Rev. B **31**, 316 (1985).
[22] H. Tanaka, T. Hasegawa, and K. Nagata, J. Phys. Soc. Jpn. **62**, 4053 (1993).
[23] T. Ono, H. Tanaka, T. Kato, and K. Iio, J. Phys.: Condens. Matter **10**, 7209 (1998).
[24] T. Ono, H. Tanaka, T. Kato, K. Nakajima, and K. Kakurai, J. Phys.: Condens. Matter **11**, 4427 (1999).
[25] D. Mukamel, Phys. Rev. Lett. **46**, 845 (1981).
[26] M. Pleimling, Eur. Phys. J. B **10**, 465 (1999).
[27] N. Shirota and H. Shiba (private communication).